JOURNAL OF MATERIALS SCIENCE 4 (1969) 471–478

Carbide Growth in a Molybdenum TZC Alloy

N. E. RYAN, J. W. MARTIN
Department of Metallurgy, University of Oxford, Oxford, UK

Received 6 December 1968

A study of the rate of growth of the carbide phase in a molybdenum–TZC alloy has been investigated over the range 1200 to 1500° C. A constant log-normal particle size distribution was maintained over the time-temperature spectrum explored. Particle growth kinetics were found which could be related to either diffusion or interface controlled processes. It is concluded that quantitative metallographic techniques are inadequate to distinguish between these mechanisms in complex alloy systems.

1. Introduction

The favourable influence of fine stable dispersions of a hard phase on the high temperature properties of metallic materials is now well established. Oxides, because of their high free energy of formation, are generally recognised as the most stable dispersions, although even these coarsen during prolonged exposure at high temperatures, with resultant deterioration of the mechanical properties of the metals containing such phases.

In the refractory metals, carbide dispersions have been shown to demonstrate [1-4] a marked strengthening influence. These carbide phases are less stable than oxide dispersions, and so their coarsening is therefore likely to be more rapid and thus influence the high temperature properties in a more profound way.

The molybdenum alloy "Mo–TZC" (so called because of the Ti(Zr, Mo) carbide it contains) has, on a strength-to-weight basis, exhibited superior properties [5] up to 1400° C to many of the more dense but higher melting tantalum alloys. Data have not been determined on the growth stability of the carbide phase which contributes to this attractive high temperature strength. The study reported here has been aimed at identifying the processes involved in the growth of the Ti (Zr, Mo) carbide in the Mo–TZC alloy in the temperature range 1200 to 1500° C, under conditions of a constant volume fraction [4, 6] of the dispersed phase.

This work has, however, demonstrated the difficulties of interpreting experimental data to provide a mechanistic explanation for growth kinetics.

2. Theoretical Background

A function to describe the rate of change in particle dimensions must take into account the relationship between the solubility (however small), size, shape and distribution of the particles and must identify the rate-controlling step (s) in the growth processes. Where particles show even small solubility, there is a tendency for the smaller particles to dissolve and the material to be deposited on the larger particles (sometimes referred to as Ostwald ripening [7]). The resultant reduction in total interfacial energy constitutes the driving force for the growth process [8, 9].

The rate of change in particle size can be controlled by the rate of transport across the particle/matrix interface or by the rate of diffusion of one or more constituents either through the matrix or by selective diffusion paths (e.g. grain-boundaries). An independent change in particle shape may also involve diffusion along the particle/matrix interface or a volume diffusion within the particle itself. Shape change could be controlled by matrix diffusion in the unlikely event of the matrix diffusion coefficient being much less than the diffusivities of the particle constituents. There is a scarcity of quantitative experimental data of particle growth in many alloy systems of practical importance.

Some studies on the growth of precipitate phases [10, 11] in nickel alloys have established clear evidence for diffusion-controlled growth. Seybolt [12] has also reviewed published data on oxide particle growth and concludes that the data are consistent with a diffusion-controlled process. In other instances, however, interface control has been postulated [13, 14] in view of the very high activation energies for oxide particle growth.

The rate of coarsening under diffusion controlled conditions has been expressed analytically by Lifshitz and Slyozov [15] and Wagner [16] as applied to particle growth in liquid media. Growth in a metallic solid solution is discussed in detail by Greenwood [9] and essentially similar formulae are derived in each case which have been reapplied in the work of Ardell and Nicholson [10, 11] to the growth of precipitate phases in nickel.

Considering a binary system containing particles of a single atomic species in a fluid matrix, the Lifshitz-Wagner equation expresses the change in volume of a spherical particle during growth by a diffusion controlled mechanism thus:

$$\bar{r}^3 - \bar{r}^3_0 = \frac{2\gamma\, DC_e\, V_m{}^2 t}{\rho^2\, RT} \qquad (1)$$

where $\bar{r}$ is the mean radius of second-phase particles at any given time t; $\bar{r}_0$ is the mean radius at $t = 0$, the time at which precipitation is complete; γ is the interfacial energy between the particle and matrix; D is the diffusion coefficient of the rate-controlling species; C_e is the concentration of diffusing element in equilibrium with a particle of infinite size; V_m is the molar volume of the precipitate; ρ is a numerical constant [9, 15, 16] which describes the distribution of particle sizes; R is the gas constant and T the absolute temperature.

With very stable dispersed phases it is reasonable to assume that the rate controlling factor should be the dissociation, association and atom transport across the particle/matrix interface. In such interface control, Greenwood [9] derives the relationship

$$\bar{r}^2 - \bar{r}^2_0 = \frac{\gamma\, DC_e\, V_m t}{\rho^2\, RT} \qquad (2)$$

In fine-grained material, preferred "pipe" diffusion along grain-boundaries can be expected to predominate at low temperatures. Such a situation may exist in dispersion strengthened materials where a polygonised sub-grain size is of comparable magnitude to the mean free path between particles. A treatment of this problem has been given for the diffusion-controlled case [17] and discussed by Greenwood [9]. The growth law in this case is given by the relationship:

$$r_f{}^4 - \bar{r}_0{}^4 = \frac{4\gamma D_g\, C_g\, V_m\, wt}{3\, AB\, RT} \qquad (3)$$

where r_0 is the initial size of a grain-boundary particle; r_f is the radius of the fastest growing particle; D_g is grain-boundary diffusion coefficient; C_g is grain-boundary solute concentration; w is the width of the grain boundary; A is a constant related to particle shape [9]. If particle volume is V, then $dV/dt = 6\pi Ar^2\, dr/dt$; B is a further constant estimated from $B \simeq \frac{1}{2} \ln (1/f)$ where f represents the fractional area of grain-boundary occupied by particles.

By expressing experimental data for particle growth in terms of equations 1, 2 and 3 it thus appears possible to identify the controlling processes in such coarsening.

3. Experimental

3.1. Material

Mo–TZC material from Climax Molybdenum Co was used. The composition was given as: titanium 1.35 wt %; zirconium 0.29 wt %; carbon 0.089 wt % and is estimated to contain approximately 1 vol % of the carbide Ti(Zr, Mo) C. The material was produced by extrusion of 4 in. diameter arc-melted ingots and swaged with intermediate anneals at 1600 and 1800° C to two different sized batches 2.5 to 3 mm diameter and 5 mm diameter with a final stress relieving treatment for 1 to 2 h at 1100 to 1150° C.

3.2. Heat Treatment

For carbide growth studies, samples of swaged Mo–TZC 1 to 1.5 cm long were annealed in vacuum (10^{-6} torr) for various times up to 250 h at 1200, 1350 and 1500° C. Each specimen was annealed only once and the same consistent batch of material was used for tests at each temperature level. Samples of 3 mm bar were used for the 1200 and 1500° C study while the 5 mm diameter material was used for particle growth study at 1350° C.

3.3. Extraction Replica Technique

Received and annealed alloy samples were first mechanically and electro-polished to produce a flat, at least 2 mm, on each sample: they were

then electro-etched in a 15% sulphuric–5% hydrochloric acid/methanol solution under identical conditions for a standard time sufficient to expose the largest particles at their mean diameter. A self-shadowing carbon (Pd) film 200 to 300 Å was evaporated on to the pre-etched samples. The evaporated carbon film was scored across to form 2 mm squares and the specimens electro-etched in a 5% hydrochloric acid/methanol solution at $< -5°$ C, washed in methanol, dried, and the carbon film floated off in distilled water.

3.4. Particle Size Analysis

Particle size measurements were made directly from the extraction replica micrographs at 5000, 10 000 and 20 000 magnifications sufficient to record 400 to 500 particles, e.g. 100 to 200 particles would be recorded on each plate at 10 000.

Particle distributions were recorded from at least three different regions along the length of each specimen.

The areal mean radii were determined by measuring particle diameters using ruled grids to classify particles into ten to twelve size ranges between 0.01 and > 1.0 μm. These measurements were accurate to within $\pm$ 0.2 mm. The results are therefore accurate within $\pm$ 0.01 μm and 0.04 μm at the respective ends of the magnification ranges used.

4. Results and Discussion

An example of the extraction replicas from which the particle size and distribution were obtained is given in fig. 1.

Since the extraction replica method may not always clearly distinguish between spherical and disc-shaped particles, thin film transmission samples were also prepared from both longitudinal and transverse cross-sections of the swaged material.

From studies [2] of carbide precipitation in molybdenum the second phase is known to form initially as plates on the {100} matrix planes. During fabrication the constraints imposed on such planar particles might be expected to give rise to preferential alignment of the dispersion. This has been observed in carbide-strengthened chromium [18]. The transmission electron-micrographs, figs. 2a and b do, however, confirm that the particles were consistently spherical in form, although a number of ellipsoidal particles were present. In addition, the transmission study

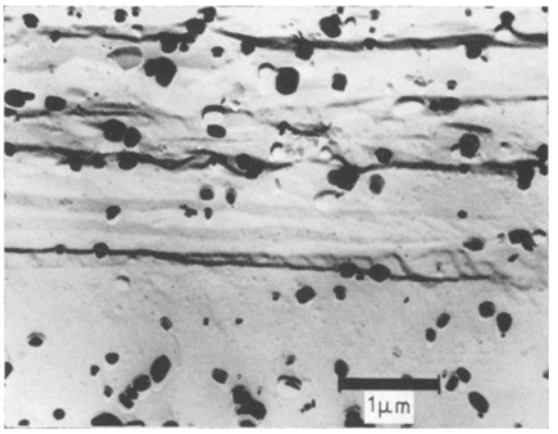

Figure 1 Carbon extraction replica of Ti(Mo,Zr)C particles in the Mo–TZC alloy.

revealed the nature of the Mo–TZC alloy structure. The alloy consisted essentially of a polygonised sub-grain structure with sub-grains 0.5 to 1.0 μm in diameter preferentially aligned with a <110> parallel to the fabrication direction.

The mean radius ($\bar{r}$) values obtained from averaging 4 to 500 particle dimensions are given in table I. The differences in the particle sizes in the as-received material for the two different batches (in the 3 mm diameter bar $\bar{r} = 0.086$ μm, in the 5 mm diameter material, $\bar{r} = 0.076$ μm), may be attributed to particle growth during the extended fabrication period for the 3 mm material over that of the 5 mm diameter batch.

The distribution of carbide particles in the form of frequency histograms were related to the predicted distributions for diffusion or interface [9] control according to the treatment suggested by Ardell and Nicholson [10]. It was noted that at longer times the particle size distribution could be imagined to relate to either of the predicted distribution curves but no clear "cut off" radius was identified. The significant particle distribution at $> 1.5\, r/\bar{r}$ may be considered to result from enhanced growth of those particles situated at or near sub-grain or grain-boundaries as, e.g. shown in fig. 3. However, using a logarithmic abscissa to plot the particle size variations the distributions were found to obey a log-normal relationship and by means of a log-probability grid [19, 20] it was noted that the initial (as-received) log-normal distribution ratio was essentially maintained during the growth processes. This is illustrated on a log-probability

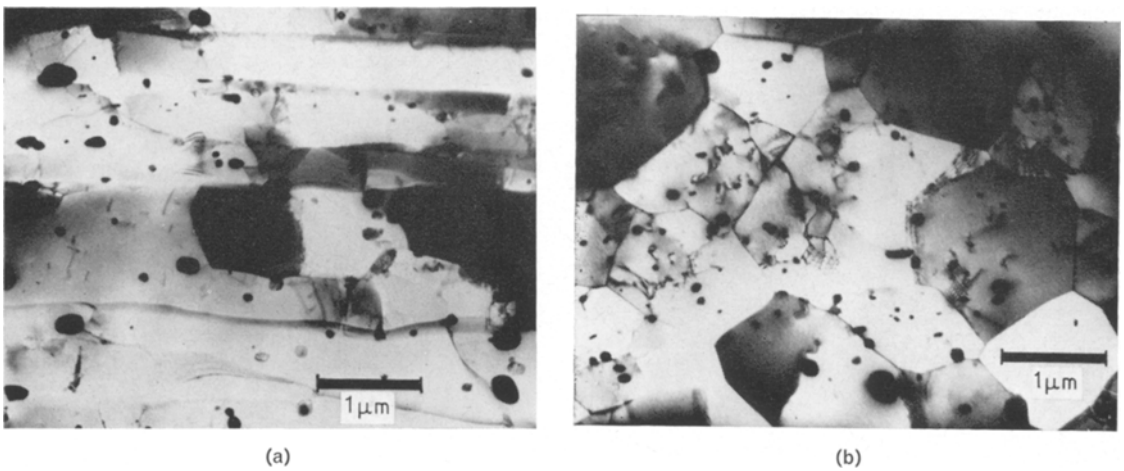

(a) (b)

Figure 2 Transmission electron micrographs of swaged stress-relieved Mo–TZC alloy: (a) longitudinal cross-section; (b) transverse cross-section.

TABLE I Tabulated data giving increase in mean particle radius r with time at 1200, 1350 and 1500° C and values of particle growth rate constants k according to diffusion or interface controlled growth laws.

Temp °C	Time h	Mean radius cm $\bar{r}/x\ 10^{-6}$	Steady state intercept on $\bar{r}^3$ versus t cm^3 × 10^{-16}	k $(\bar{r}^3 - \bar{r}^3_0)/h$ cm^3 × 10^{-18}	Steady state intercept on $\bar{r}^2$ versus t cm^2 × 10^{-12}	k $(\bar{r}^2 - \bar{r}^2_0)/h$ cm^2 × 10^{-15}
	0	8.6				
1200	5	9.1	8.5	3	88.5	22
	12.5	9.6				
	100	10.6				
	250	11.6				
	0	7.6				
1350	2.5	8.6	6.9	6.8	81.0	41
	5	9.0				
	22	9.6				
	67	10.5				
	108	11.3				
	0	8.6				
1500	1	9.5	10.6	15.1	103	87
	2.5	10.3				
	14	10.8				
	27	11.4				
	54	12.3				

grid in fig. 4 where the particle size distributions after 250 h at 1200° C and 54 h at 1500° C remain almost parallel with the initial particle size distribution.

5. Plotting Particle Size Data

The derivation of equation 1 assumes that the particle growth rate is controlled by a diffusion process and $\bar{r}$ becomes proportional to $t^{1/3}$, or $\bar{r}^3$ to t which is equivalent to volume change with time. The values recorded in table I are plotted in fig. 5 as $\bar{r}^3$ versus t where a linear relation, after a certain incubation period, is obtained. Plotting data according to the $\bar{r}$ versus $t^{1/3}$ form is only considered appropriate when $\bar{r}_0 \simeq 0$ or when $\bar{r} \gg \bar{r}_0$ i.e. when large growth rates are observed. The incubation period, decreasing with increasing temperature, observed when the results are plotted as $\bar{r}^3$ versus t may be considered as the time required to establish an equili-

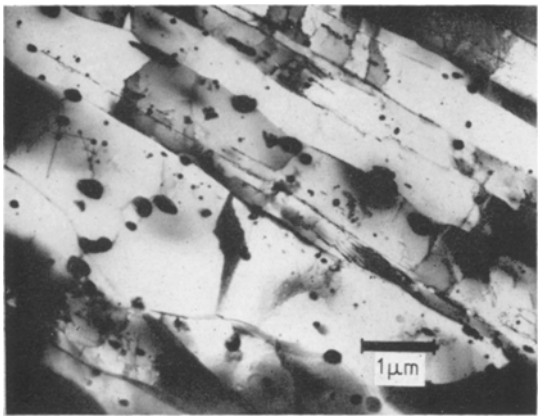

Figure 3 The increase in the size of particles situated at or near sub-grain-boundaries. Transmission electron micrograph.

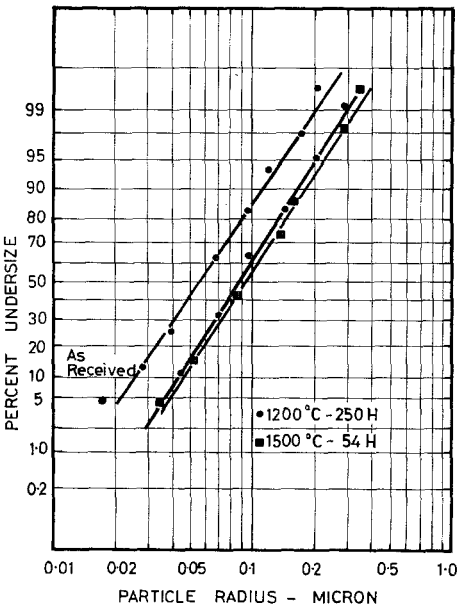

Figure 4 Log-normal distribution of carbide particle sizes plotted on a log-probability grid.

brium structural condition associated with an initial rapid growth rate. The decrease in incubation time with increasing temperature is consistent with this explanation and has been observed by Cook and Nutting [21] investigating the influence of strain on the growth rate of Cu Al_2 in an aluminium–4% copper alloy. An initial rapid growth period related to the degree of prior strain occurred before an $\bar{r}^3$ versus t "steady state" diffusion-controlled growth was recorded.

The intercept at t_0 yields approximate values of $\bar{r}_0^3$ (see table I). Although strictly speaking $\bar{r}_0$ is at time t, after the attainment of equilibrium

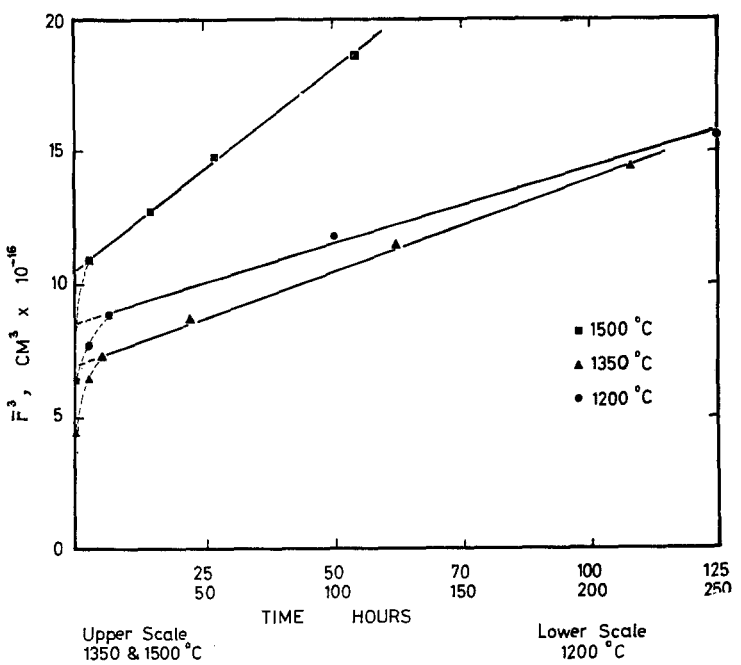

Figure 5 Increase in mean particle size plotted according to $\bar{r}^3$ versus t.

the time is small compared to the annealing time and has been neglected in the assessment of the rate constant k given by the slope of $\bar{r}^3$ versus t. Calculated values of k and $\bar{r}^3$ are listed in table I.

These data were used to obtain a plot of log $(\bar{r}^3 - \bar{r}_0^3)$ versus log t and as might be anticipated from fig. 5 a straight line relationship with a slope of unity was obtained, according to the prediction of the diffusion-controlled growth law (equation 1).

If it is assumed that γ is essentially independent of temperature equation 1 may be written:

$$\frac{\bar{r}^3 - \bar{r}_0^3}{t} = \frac{C_e}{T} D_0 \exp - \frac{Q}{RT}(\beta) \qquad (1a)$$

where $\beta = 2\gamma/\rho^2 . V_m^2/R$, D_0 = the frequency factor related to D the diffusion coefficient of the rate controlling species and Q = the activation energy associated with the growth process. Thus if no significant change in the solubility occurs below 1500° C, as indicated by Chang [4] and by recent solubility estimates [6], we may assume C_e is constant over the temperature range in question and the activation energy associated with the growth process may then be estimated from the slope of a plot of log kT against $1/T$, where k (given in table I) is the slope of the $\bar{r}^3$ versus t plots. The data plotted according to the above expression (1a) in fig. 6 gave a value of 32 kcal/mole. This value is substantially less than values for the activation energy of molybdenum self-diffusion [22], 92 kcal/g atom or the diffusion of titanium in molybdenum [23], 101.5 kcal/g atom. A value of 29 kcal/g atom, for the diffusion of carbon in molybdenum has been quoted by Samsonov and Epik [24] and 31 kcal/g atom by Gibala and Wert [25] using internal friction methods. Although higher values (35.5 to 41 kcal) have been obtained by other workers [26-28], it is concluded that the data obtained here are consistent with a diffusion-controlled growth process depending essentially on the diffusion of carbon. By taking values quoted for the carbon diffusion coefficients D_0 and D [24, 27, 28] and reported data for the solubility of carbon [28] in molybdenum, and substituting in equation 1, values for the interfacial energy (γ) ranging between 150 and 5000 ergs/cm^2 were obtained.

The data quoted above have been obtained by assuming initially the operation of a diffusion controlled growth process. Growth kinetics according to interface control can equally be justified if we consider the requirement of interface dissociation of the stable carbide phase as the rate controlling factor; thus a linear relationship between $\bar{r}^2$ versus time might be anticipated. A plot of $\bar{r}^2$ versus t is shown in fig. 7 and again a reasonable straight line relationship is displayed following an initial rapid growth incubation period. Values for $\bar{r}_0^2$ were obtained from the intercept at t_0 and the progressive change in particle surface area plotted in the form log $(\bar{r}^2 - \bar{r}_0^2)$ versus log t gave a slope of unity, apparently confirming an interface-controlled growth law. An estimate of the activation energy value for interface control gave a value of 28.5 kcal/mole, (log kT versus $1/T$). The energy required to remove atoms from the TiC lattice might be expected to be of the same order as the free energy of formation of the TiC phase. In the standard state this energy is of the order — 40 kcal/mole [29] but the departure from standard state conditions by the formation of the phase in dilute solution would be expected to lower this value (i.e. to make it more positive). The magnitude of this reduction is dependent upon the activities of the second phase and its constituents in molybdenum [29], but the effect will tend to bring the value of the free energy of formation of the phase closer to that of the activation energy observed here for an assumed interface-controlled growth process.

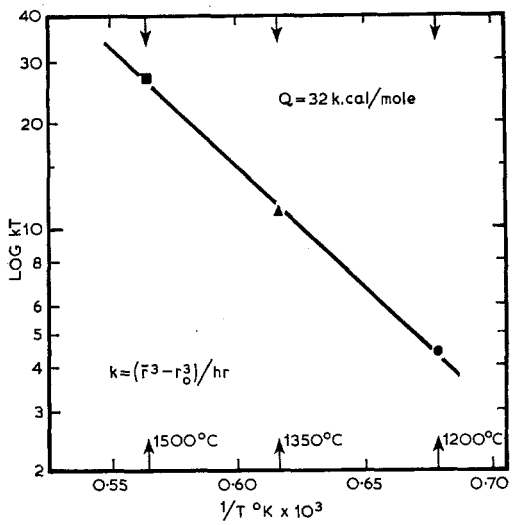

Figure 6 Plot of log kT against reciprocal of the absolute temperature, $1/T$ where $k = (\bar{r}^3 - \bar{r}_0^3)/h$. The slope indicates an activation energy of 32 kcal/mole.

In a study of the growth of manganese particles in magnesium, Smith [30] was also unable to distinguish between diffusion and

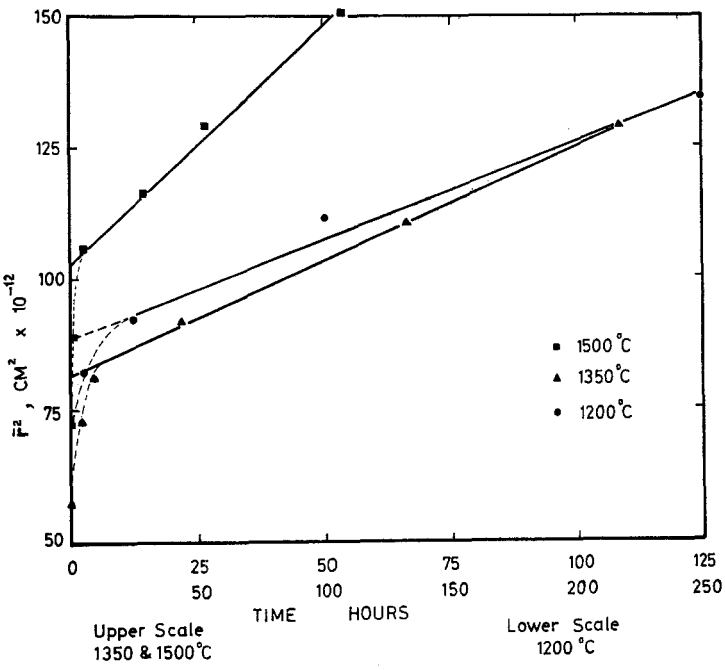

Figure 7 Increase in particle size plotted as $\bar{r}^2$ versus time.

interface-controlled growth. He showed that particle growth data could be plotted equally well according to either diffusion- or interface-controlled growth kinetics.

It might be further argued that the fine sub-grain structure, which persisted in these Mo–TZC alloy samples [31] for up to 200 h at 1200° C and for ~ 20 h at 1500° C, might provide a short circuit sub-grain boundary diffusion path. An interparticle spacing of ~ 2 to 3μm compared with a sub-grain size of ~ 1μm suggests that a major fraction of the dispersed particles must therefore lie on (e.g. fig. 3) or very near to these sub-grain-boundaries.

In such circumstances the particle growth might be expected to vary linearly with time according to the fourth power of the average particle radius, equation 3. By plotting $\bar{r}^4$ against time, a linear relationship was again obtained.

This situation demonstrates the difficulties which must be faced in plotting experimental data in order to satisfy some predetermined or assumed relationship.

Over the temperature range (1200 to 1500° C) used in this study it is considered that bulk diffusion is likely to be more important than preferred grain-boundary diffusion, so that the latter model is not considered appropriate. A linear relation between $\bar{r}^4$ and t cannot therefore be regarded as a valid criterion for establishing the rate-controlling process.

The initial rapid growth observed in this study has been attributed to a high dislocation density present in the swaged Mo–TZC before a stable sub-structure was completely established [31].

6. Conclusions

(i) The measured coarsening rate for the growth of the carbide phase in the Mo–TZC alloy is in accordance with theories based on interfacial processes or on bulk diffusion processes.

(ii) On the basis of control by bulk diffusion, the observed activation energy (Q = 32 kcal/mole) compares well with quoted values for the activation energy for carbon diffusion in molybdenum.

(iii) On the basis of control by interfacial transport, the activation energy (Q = 28.5 kcal/mole) can be approximated to the free energy of formation of TiC in dilute solution in molybdenum but the complex composition of the Mo–TZC carbide phase makes it impossible to compare directly with a theoretical model.

(iv) Metallographic kinetic studies of this kind,

do not appear to provide a simple means of distinguishing rate controlling growth processes in *complex* alloy systems.

Acknowledgement

The authors express their appreciation to Professor P. B. Hirsch FRS for the provision of laboratory facilities and NER, on leave from the Aeronautical Research Laboratories, is indebted to the Public Service Board of the Commonwealth of Australia for support under the terms of a Postgraduate Scholarship.

References

1. G. M. AULT, 1965 Gillette Memorial Lecture, ASTM April 1966.
2. N. E. RYAN and J. W. MARTIN, 6th Plansee Seminar 1968 Metallwork Plansee, Reutte, Austria (to be published).
3. F. OSTERMAN, *ibid.*
4. W. H. CHANG, *Trans. ASM* **57** (1964) 525.
5. J. C. SAWYER and E. Y. STEIGENWALD, *J. Matls.* **2** (1967) 341.
6. N. E. RYAN and J. W. MARTIN, *J. Less Comm. Met.* (1969) (to be published).
7. R. A. ORIANI, *Acta Metallurgica* **12** (1964) 1399. (W. OSTWALD, *Z. Physikal Chem.* **34** (1900) 495).
8. G. W. GREENWOOD, *Acta Metallurgica* **4** (1956) 243.
9. G. W. GREENWOOD, Proceedings of Manchester Conference on Phase Transformation in Crystalline Solids, Inst. Metals (to be published)
10. A. J. ARDELL and R. B. NICHOLSON, *Acta Metallurgica* **14** (1966) 1295. *J. Phys. Chem. Solids* **27** (1966) 1793.
11. A. J. ARDELL, [9]
12. A. U. SEYBOLT, G. E. Co. Research and Development Centre, Schenectady NY Rept. No. 66, CO68.
13. J. A. DROMSKY, F. V. LENEL, and G. S. ANSELL, *Trans. Met. Soc. AIME* **224** (1962) 236.
14. N. KOMATSU and N. J. GRANT, *ibid* **230** (1964) 1090.
15. I. M. LIFSHITZ and V. V. SLYOZOV, *J. Phys. Chem. Solids* **19** (1961) 35.
16. C. WAGNER, *Z. Elektrochem.* **65** (1961) 581.
17. M. V. SPEIGHT, *Acta Metallurgica* **16** (1968) 133.
18. N. E. RYAN, *J. Less Comm. Met.* **11** (1966) 221.
19. C. ORR and J. M. DALLAVALLE, "Fine Particle Measurement" (Macmillan Co, NY, 1959).
20. C. ORR, "Particulate Technology" (Macmillan Co, NY, 1966).
21. J. D. COOK and J. NUTTING, [9].
22. J. ASKILL, "Diffusion in the BCC Metals" (American Society for Metals, 1965) p. 247.
23. P. G. SHEWMAN and J. H. BECHTOLD, *Acta Metallurgica* **3** (1965) 452.
24. G. V. SAMSONOV and A. P. EPIK, *Phys. Metals and Metallog. (USSR)* **14** (3) (1962) 144.
25. R. GIBALA and C. A. WERT, "Diffusion in the BCC Metals" (American Society for Metals, 1965) p. 131.
26. II SPIVAK, *Phys. Metals and Metallog. (USSR)* **22** (6) (1966) 52.
27. A. I. NAKONECHNIKOV, L. V. PAVTINOV, and V. N. BYKOV, *ibid* **22** (2) (1966) 73
28 P. S. RUDMAN, *Trans Met. Soc. AIME* **239** (1967) 1949.
29. F. D. RICHARDSON, *J. Iron and Steel Inst.* **175** (1953) 33.
30. A. F. SMITH, *Acta Metallurgica* **15** (1967) 1867.
31. N. E. RYAN, unpublished.